PS/DL/LEAR/Note 81-12
Décembre 1981

ELECTROSTATIC SEPARATION OF p-$\bar{p}$ COLLIDING BEAMS IN LEAR

M. Conte* and D. Möhl

* ISF Università di Genova, Italy
INFN Sezione di Genova, Italy

1. INTRODUCTION

In order to obtain a short p-$\bar{p}$ collision region[1] in LEAR, the possibility of having the two beams cross, rather than to have head-on collisions of short bunches[2] is going to be investigated.

Separation and crossing of the two counter-rotating beams can be obtained by electrostatic fields, which provide closed-orbit distortions symmetrical with respect to the unperturbed orbit. An orbit distortion of the p beam is accompanied by a closed-orbit deviation of opposite sign for the $\bar{p}$ beam.

The harmonic content of such a perturbation has to be chosen, subject to the limitation on space available for electrostatic deflectors and subject to the aperture available for the two beams.

The arrangement sketched in Fig. 1 has been chosen after studying other possible schemes. Note that horizontal deflection plates are introduced at the entrance or exit blocks of the magnets, where space could in principle be made available. Four magnet blocks are involved in the scheme studied.

2. CLOSED-ORBIT PATTERN

For LEAR with a low beta insertion in straight section 2 giving $\beta_H = \beta_V = 1$ m, the horizontal betatron function[3] β_H results as given in Fig. 2a, where β_H is plotted versus the Courant-Snyder angle[4] $\phi = \int \frac{ds}{Q_H \beta_H(s)}$ and in Fig 2b, where β_H is plotted versus the machine azimuth θ. The relation between ϕ and θ is drawn in Fig. 3. The origin of ϕ and θ has been chosen to coincide with the centre of SL4 (position of the RF cavities - see Fig. 1).

According to Courant-Snyder[4] the closed-orbit distortion is conveniently expressed in terms of the normalized variable η which is related to the deviation of the orbit, $x_{c.o.}$, by

$$x_{c.o.} = \eta \, \beta_H^{\frac{1}{2}} \tag{2.1}$$

As shown in 4), η is the solution of the following equation

$$\frac{d^2\eta}{d\phi^2} + Q_H^2 \, \eta = Q_H^2 \, f(\phi) \qquad (2.2)$$

where in our case the "driving function" $f(\phi)$ is

$$f(\phi) = \frac{\bar{\beta}_H^{3/2}}{\pi d_H} \, \frac{U_D}{U_P} \, \frac{1}{\beta^2\gamma} \sum_{m=1}^{\infty} (-1)^{m+1} \sin m \frac{5\pi}{6} \sin m\phi \qquad (2.3)$$

Here:

$\bar{\beta}_H$ = value of β_H evaluated in the deflector regions
d_H = half-distance between left and right deflection plates
U_D = deflector voltage
U_P = 938 MV
$\beta\gamma$ = relativistic parameters

Notice that the Fourier expansion of the deflections corresponding to Fig. 1 has been obtained by considering an azimuthal function which consists of four narrow rectangular functions, the first couple being positive and the second one negative as shown in Fig. 4.

The solution of eq (2.2) is

$$\eta = Q_H^2 \, \eta_o \sum_{m+1}^{\infty} \frac{(-1)^{m+1}}{Q_H^2 - m^2} \sin m \frac{5\pi}{6} \sin m\phi \qquad (2.4)$$

with

$$\eta_o = \frac{\bar{\beta}_H^{3/2}}{\pi d_H} \, \frac{U_D}{U_P} \, \frac{1}{\beta^2\gamma} \qquad (2.5)$$

Combining equations (2.1) and (2.4) one has a closed-orbit distortion as shown in Fig. 5.

3. CROSSING ANGLE

One concludes from Fig. 5 that the closed orbit has a maximum deviation in straight sections 1 and 3. We take the available aperture there to be limited to ± 55 mm. With some allowance for beam size and orbit imprecision this permits a maximum separation of the two beam centres by, say, 2 x 40 mm (Fig. 6).

We now calculate the resulting crossing angle in straight section 2.

From (2.4) and (2.1) we find that the maximum orbit distortion occuring for $\phi \simeq 75^o$, $\beta_H = 10.5$ m is

$$\frac{\hat{x}_{c.o.}}{Q_H^2\ \eta_o} = 3.7 \quad (m^{\frac{1}{2}})$$

In a similar way we find that in the centre of LS2 ($\phi = 180^o$, $\beta = 1$ m)

$$\frac{\psi}{Q_H \eta_o} \simeq \frac{x'_{c.o.}}{Q_H^2\ \eta_o} = 0.74 \ (m^{-\frac{1}{2}})$$

and hence

$$\frac{\psi}{\hat{x}_{c.o.}} = \frac{0.74}{3.7} \qquad (m^{-1})$$

$$\psi = \frac{0.74}{3.7} \times 40 \ (mrad)$$

$$\boxed{\psi \simeq 8 \ mrad}$$

In other words the available aperture limits the crossing angle obtainable in our scheme to a maximum of 8 mrad. The corresponding voltage on the deflection plates can be worked out from (2.5), assuming a separation of the plates by 2 x 25 mm (see Fig. 7).

Equations (2.4) and (2.5) give

$$U_D = \eta_o \frac{\pi \, d_H}{\bar{\beta}_H^{3/2}} \beta^2\gamma \, . \, 938 \text{ MV}$$

where d_H = 25 mm (plate half separation)

$\bar{\beta}_H$ ≃ 5 m (focusing function at plate location)

$\beta^2\gamma$ = 1.93 at 2 GeV/c

$Q_H^2 \, \eta_o = 10^{-2}$ from (2.5) for $x'_{co} = \psi = 8$ mrad in the centre of LS2

and Q_H ≃ 2.4 (horizontal betatron wave number)

Inserting these numbers we find

$$U_D = \pm 21 \text{ kV}$$

which seems feasible.

A plate separation as small as possible had to be chosen so that the field is radial rather than to go from the plates (potential $\pm U_D$) to the chamber (potential 0). As the height is 55 mm, a total of 50 mm as assumed above is already at the limit of the desirable. On the other hand, the plates heavily restrict the aperture and have to be withdrawn for normal operation and perhaps even during injection and preparation of the beams for the collisions. An alternative design of the horizontal deflection plates is sketched in Fig. 8. It leaves practically the full horizontal aperture at the expense of some reduction in the vertical acceptance. However, as the field lines are no longer parallel at the beam position, the resulting non-linear lens action may blow up the beam.

Having another look at Fig. 5, we note that the large beam separation in LS3, where electron cooling[5)] is going to be installed, is advantageous in that it may facilitate independent cooling of the two beams.

Finally, we note from Fig. 5 that in the scheme adopted coasting beams would cross in 4 places. To avoid beam interaction in the two unwanted places (BH1, BH2), it is necessary to have bunched beams with a bunch length not exceeding twice the distance between the main and the parasitic crossing point, i.e. $\ell_{bunch} \lesssim 24$ m (total bunch length). This can be achieved with a lower RF voltage then needed for the 5 m bunches contemplated in the design report (about 2 kV instead of 50 kV, assuming $\Delta p/p = \pm 10^{-3}$ for the bunched beams in both alternatives).

4. BEAM PROPERTIES MATCHED TO THE AMMAN-RITSON LIMIT

Starting from the relation for the beam-beam tune shift[2,6]

$$\Delta\nu = r_p \frac{N \beta_V}{4 A_{int}} \left(\frac{1 + \beta^{-2}}{\gamma}\right)$$

we work out the required interaction area (ref 2. 6).

$$A_{int} = \frac{\pi}{4} a_v \quad (a_H^2 + \ell^2 \psi^2)^{\frac{1}{2}}$$

We take

ψ = 8 mrad

β_V = 6 m

N = 6×10^{11}

β = 0.905 $\quad\gamma$ = 2.35 (2 GeV/c)

r_p = 1.54×10^{-18} m

Examples of resulting sets of parameters are given in Table 1. The interaction length ℓ is related to horizontal beam size and crossing angle by

$$\ell = 2 a_H/\psi$$

Note that for the evaluation of the Amman-Ritson limit, the beam parameters referring to the second crossing region (SL4) have been taken where, for reasons of space available, the beta function cannot be much reduced beyond 6 m. However, the interaction length ℓ^* (last column of Table 1) and the luminosity refer to the main intersection (LS2).

$\Delta\nu$ (assumed)	a_H in LS4 (mm)	$\ell = \frac{2a_H}{\psi}$ at $\beta_H = 6$ m (m)	$a_{eff} = (a_H^2 + \ell^2\psi^2)^{\frac{1}{2}}$ (mm)	a_V (mm)	E_V (π mm.mrad)	E_H (π mm.mrad)	$\mathcal{L}$ in LS2 ($cm^{-2}s^{-1}$)	ℓ^* in LS2
a) 5×10^{-2}	8	1	17	1.8	0.6	5	2.5×10^{30}	1.0
b) 5×10^{-3}	20	2.3	44	6.9	9.6	80	2.5×10^{29}	2.3
c) 5×10^{-3}	10	1.3	22	13.0	33.0	20	1.1×10^{29}	1.3

a) very strong cooling of both beams to counteract beam-beam effect at $\Delta\nu = 5 \times 10^{-2}$ necessary

b) case with large E_H, small E_V

c) case with small E_H, large E_V

Intermediate cases are possible.

Table 1: Examples of parameters resulting from design to the Amman-Ritson limit

The assumed tune shift of 5×10^{-2} (first line) requires very strong electron cooling to counteract the beam blow-up whereas the second and third cases have the (canonical) $\Delta\nu = 10^{-3}$. In the first case the matched beam size is extremely small, especially in the vertical plane and thus the beam may be prone to all sorts of blow-ups (e.g. intra beam scattering).

The second and third cases turn out to give more or less the same beam properties as worked out for head-on collisions in the design report except that the interaction length is reduced.

As the enhancement of the beam-beam limit by cooling is a subject on which no direct experimental data exist and since the theory of the beam-beam effect is still under development and to some extent controversal, we feel that the tolerable $\Delta\nu$ has to be determined empirically once high energy e-cooling of both beams is available.

5. BEAM DENSITY LIMITATION

We now want to work out two limits related to the number of circulating particles for the beam characteristics found before: the space-charge tune shift, known as Laslett detuning[7], and the threshold for the microwave instability due to beam environment interaction (Keil-Schnell limit with local values for current and momentum spread).

For a ribbon-like beam, with an elliptical cross-section of half-width $a = a_H$ and half-height $b = a_V$, the appropriate tune shift[7] formula is

$$|\Delta Q_V| = \frac{N r_p}{B_f} \frac{\beta_V}{\pi b (a+b)} \frac{1}{\beta^2 \gamma^3} \tag{5.1}$$

where all quantities have been defined in the previous section. Referring to Table I (row with $\Delta\nu = 5 \times 10^{-2}$), one has $a = 8$ mm, $b = 1{,}8$ mm, $\ell_{bunch} \leq 20$ m, i.e. $B_f \simeq \frac{2}{\pi} \frac{20}{78.5} = 0.17$ (where the factor $2/\pi$ accounts for the higher density in the bunch centre). These are the beam properties in LS4 but they also represent, to a good approximation, averages over the circumference. We then have

$$|\Delta Q_V| \simeq 0.046 \quad \text{at} \quad 2 \text{ GeV/c}$$

Although accelerators can work with Laslett tune shifts up to 0.25 we do not know whether long term stability in a storage ring can be assured with a ΔQ of 0.05.

The stability criterion against microwave instability for a bunched and/or coasting beam is given[8] by

$$\left|\frac{Z_n}{n}\right| \leq B_f \frac{2\pi R\, U_p}{N\, e\, c}\, \beta\, \gamma\, |\eta| \left(\frac{\Delta p}{p}\right)^2 \tag{5.3}$$

where not yet defined quantities are

$|Z_n|$ = modulus of beam equipment coupling impedance at frequency $n\, f_{rev}$, $|Z_n/n| \geq 100\ \Omega$ will be taken for LEAR

$2\pi R$ = LEAR circumference = 78.54 m

e = electron charge = $1.6\ 10^{-19}$ C

c = speed of light = 2.998×10^8 m/s

$|\eta|$ = modulus of the "off energy function" = $\frac{1}{\gamma^2} - \frac{1}{\gamma_{tr}^2}$ = 0.18 for LEAR operating at 2 GeV/c

$\left(\frac{\Delta p}{p}\right)$ = minimum momentum spread allowed, to be evaluated.

Hence, for a bunch of less than 20 m, i.e. $B_f \leq 0.17$ as before, one requires $\Delta p/p \geq 10^{-3}$ at 2 GeV/c.

Intra beam scattering - another important density limitation - needs further study.

6. CONCLUSIONS

We have investigated a scheme using electrostatic separation of the two beams with an horizontal cross-over to create a well localized interaction region. The available aperture limits the crossing angle obtainable to 8 mrad.

The deflection plates have to be put close to the centre of the chamber to create a proper deflection field. This will drastically restrict the acceptance of the machine. A solution to be considered seems to have plates which are retractable by remote control and which are moved out of the useful aperture during normal machine operation and probably even during injection and beam preparation for the collider mode.

The interaction length and the luminosity obtainable depend strongly on the permissible beam-beam tune shift. With the canonical $\Delta\nu = 5 \times 10^{-3}$ matched beam properties similar to the "design report case"[2)] result.

If it is possible to work with higher tune shifts and compensate the blow-up by strong electron cooling of both beams, then a substantially shorter interaction region seems feasible on paper. To obtain the corresponding higher luminosity, extremely small beam size (dense beams) is required, with the danger of various sorts of beam blow-up.

The problems of injection, stacking, cooling and acceleration of the beams for the collider mode have not been treated but will definitely require great attention. The reduction of the aperture by the deflector plates looks uncomfortable in this context.

REFERENCES

1. P. Dalpiaz et al, IV European Antiproton Symposium, Ed. Friedman, Editions du CNRS (1978), p. 689-695 - Vol. II.

   P. Dalpiaz, CERN $\bar{p}$ LEAR Note 55 (1977).

2. G. Plass ed., CERN/PS/DL 80-7 (1980), Chapters 6-9.

3. J. Jäger, PS/DL/LEAR/Note 80-1 (1980).

4. E.D. Courant and H.S. Snyder, Ann. Phy. 3,1 (1958).

5. U. Bizzari, M. Conte, L. Tecchio and A. Vignati, submitted for publication in N. Cimento (1982).

6. M. Sands, SLAC Report 121 (1970).

7. L.J. Laslett, BNL Report 7534 (1963).

8. W. Hardt, IXth. Int. Conf. on High Energy Accel., Proceedings, p. 434 (1979).

   D. Boussard, CERN Lab Report II/RF/Int./75-2 (1975).

   W. Schnell, 1975 ISABELLE Summer Study, July 14-15, Proceedings Vol. I, p. 126 (1975).

Distribution

LEAR Liaison Group
LEAR Design Committee
U. Gastaldi EP
K. Kilian EP
H. Poth EP

/ed

Figure captions

Fig. 1 LEAR general layout and location of horizontal orbit deflection electrostatic plates

Fig. 2a Plot of the horizontal betatron function β_H versus

$$\phi = \int \frac{ds}{Q_H \beta_H(s)}$$

Fig. 2b Plot of the horizontal betatron function β_H versus the LEAR azimuth θ

Fig. 3 Connection between ϕ and θ

Fig. 4 Azimuthal distribution of the electrostatic perturbation

Fig. 5 Closed orbit pattern

Fig. 6 Sketch of the chamber and the two separated beams in SL1 (schematic)

Fig. 7 Sketch of separation plates and beams in magnet blocks BH1, 2 (schematic)

Fig. 8 Alternative design of separation plates to save horizontal acceptance (at the expense of vertical aperture)

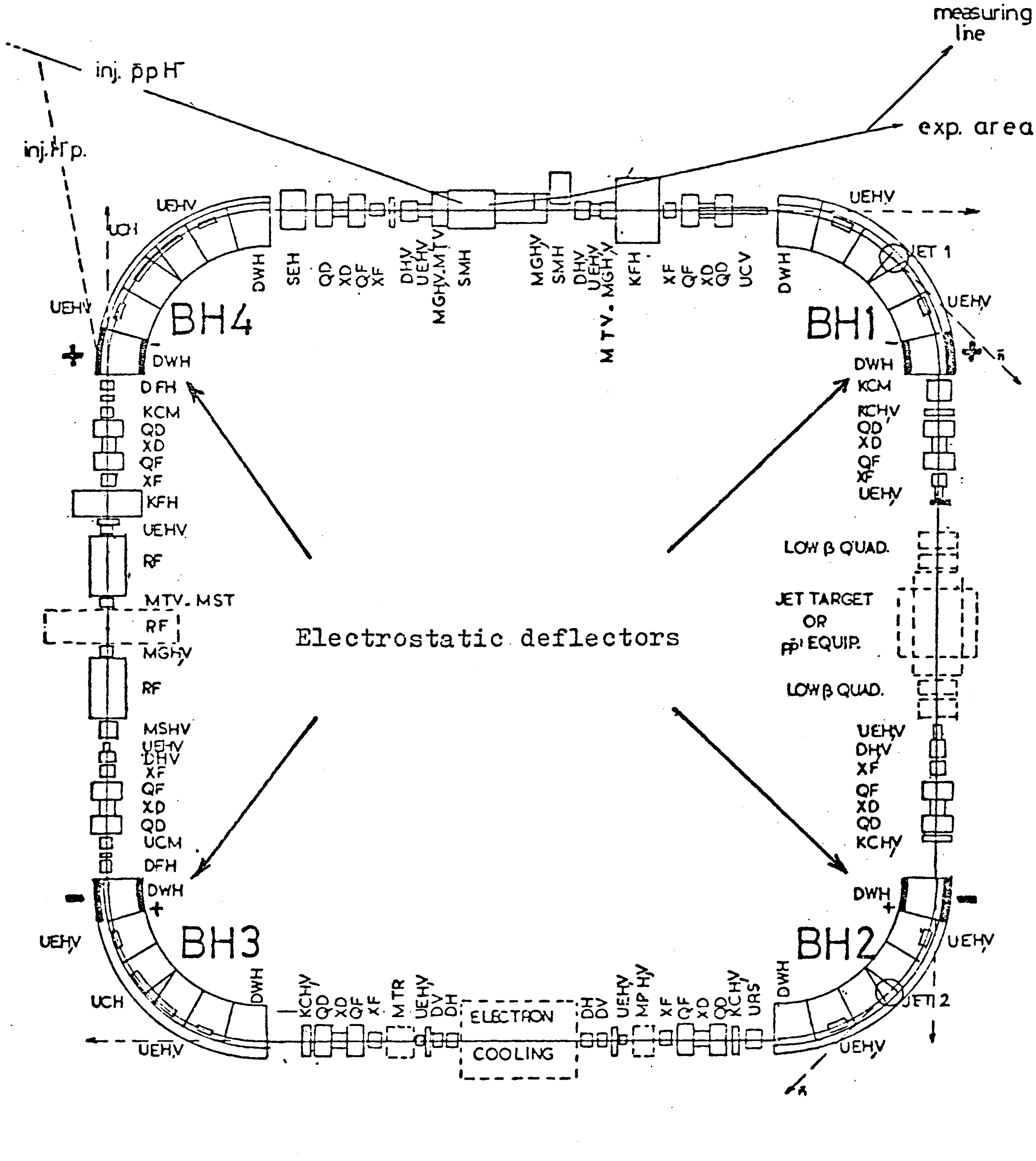
measuring line
inj. p̄pH⁻
exp. area
inj. H⁻p.
BH1
BH2
BH3
BH4
Electrostatic deflectors
JET 1
JET 2
LOW β QUAD.
JET TARGET OR p̄p EQUIP.
ELECTRON COOLING

Fig. 1

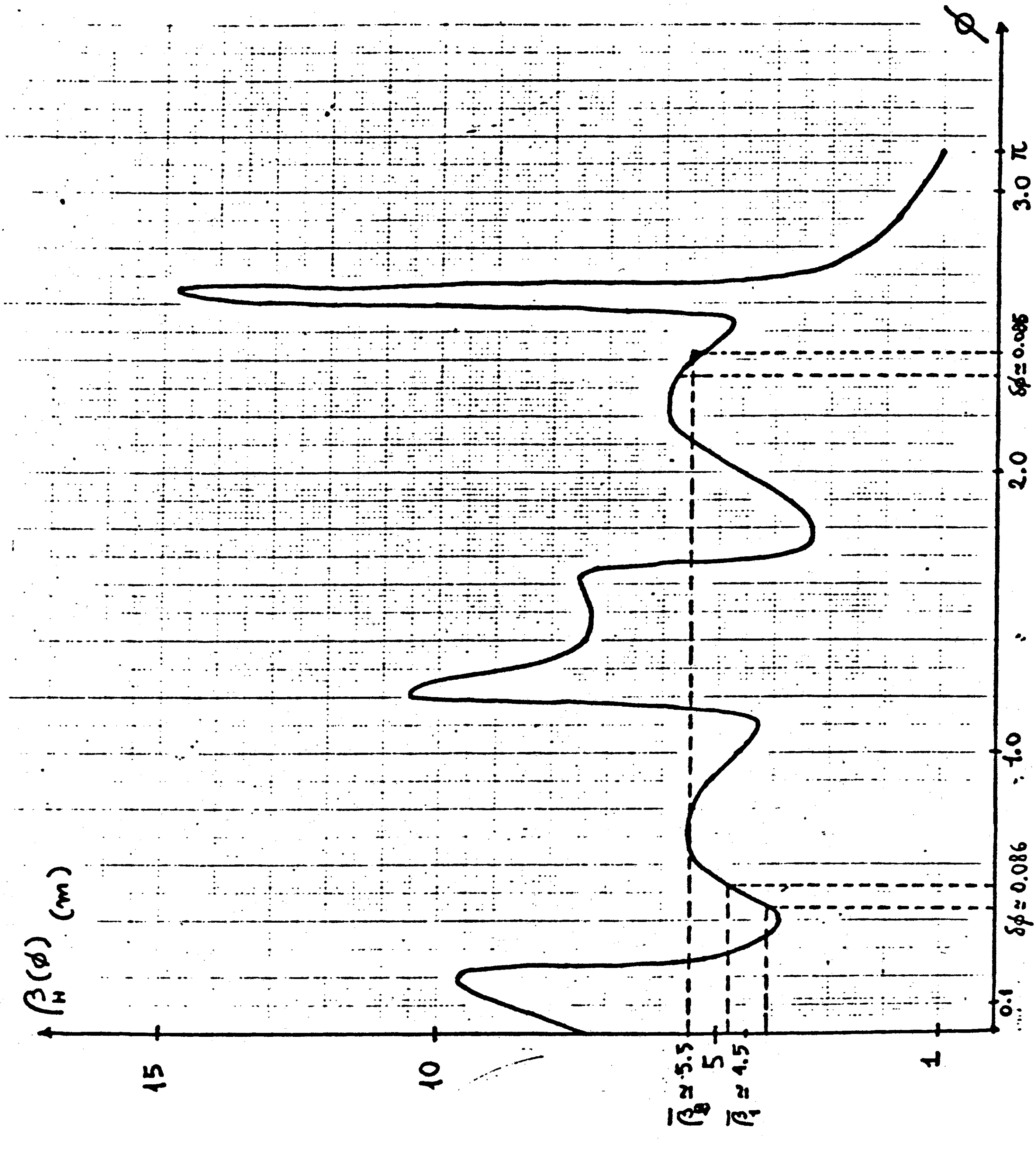

Fig. 2a

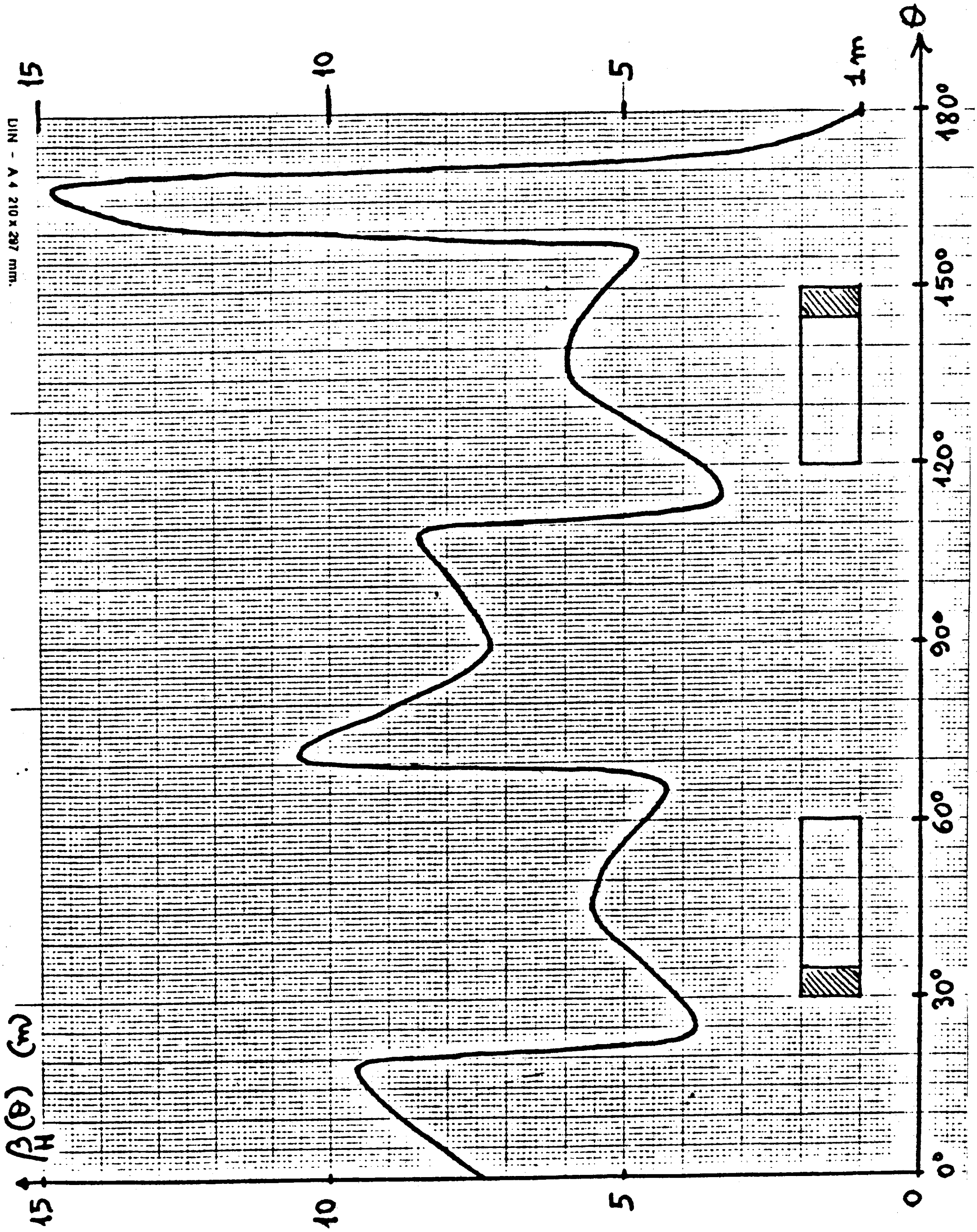

Fig. 2b

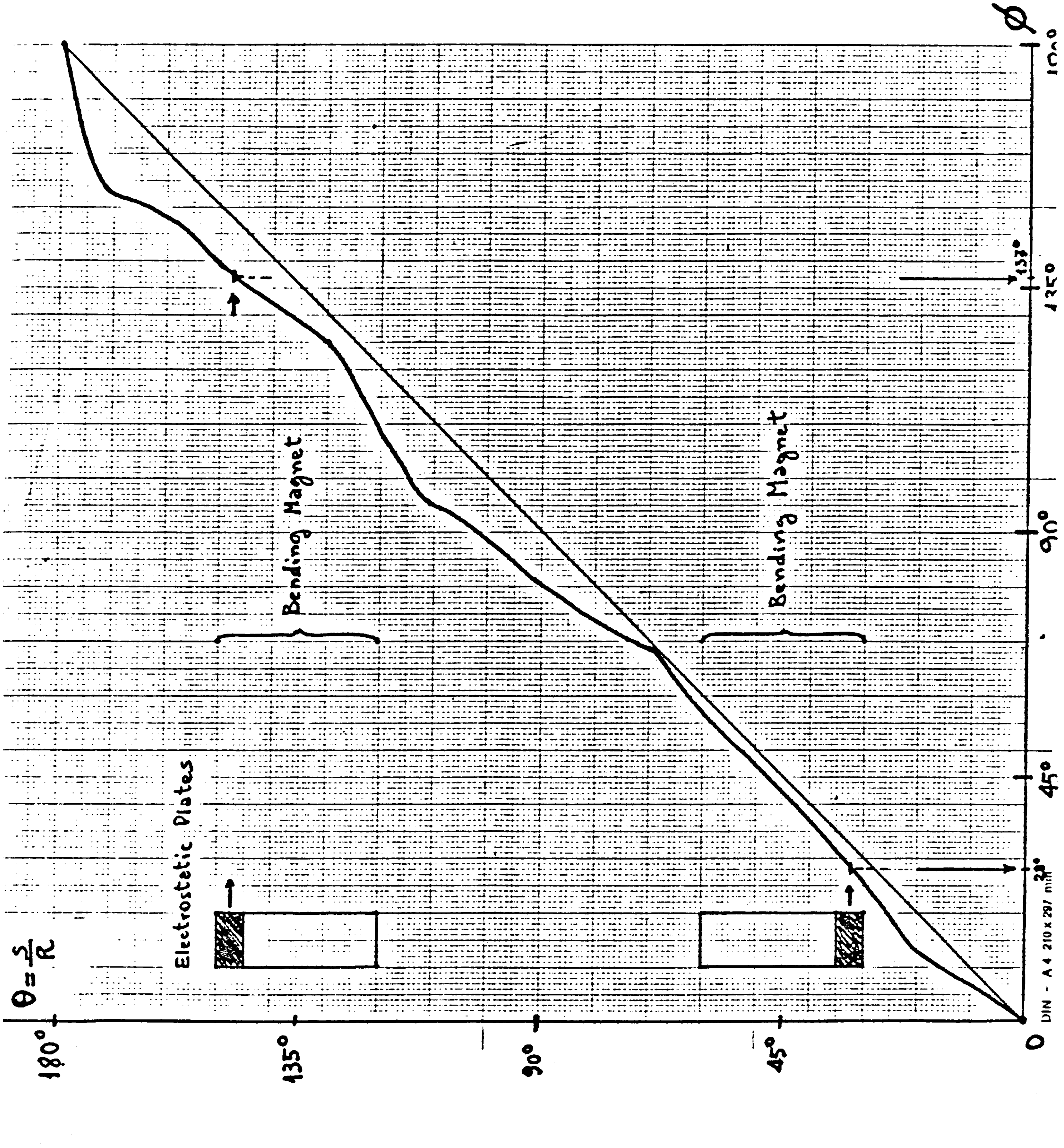

$\theta = \frac{s}{R}$
Electrostetic Plates
Bending Magnet
Bending Magnet
180°
135°
90°
45°
0
ϕ
45°
90°
135°
157°
28°
DIN - A 4 210 x 297 mm

Fig. 3

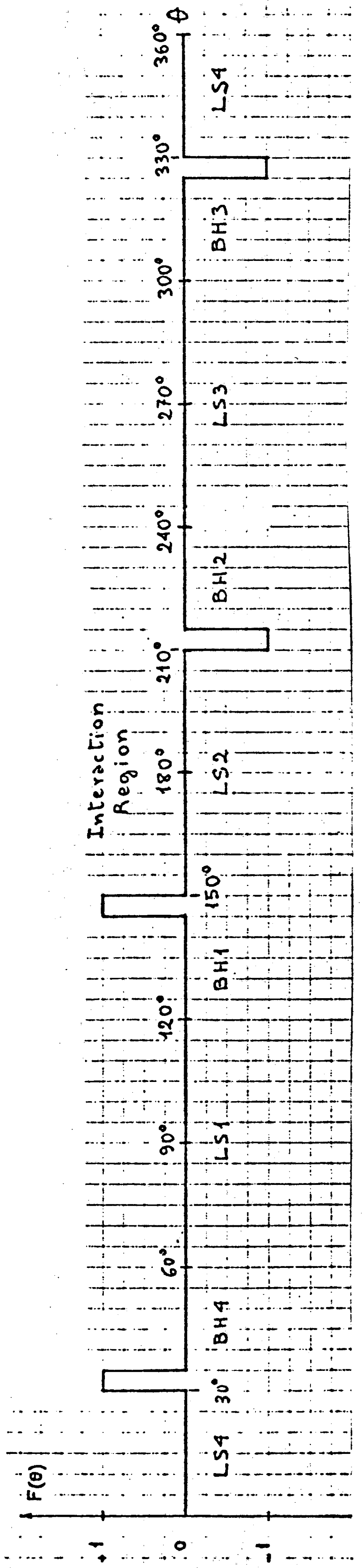

F(θ)
θ
+1
0
-1
30°
60°
90°
120°
150°
180°
210°
240°
270°
300°
330°
360°
LS4
BH4
LS1
BH1
LS2
BH2
LS3
BH3
LS4
Interaction Region

Fig. 4

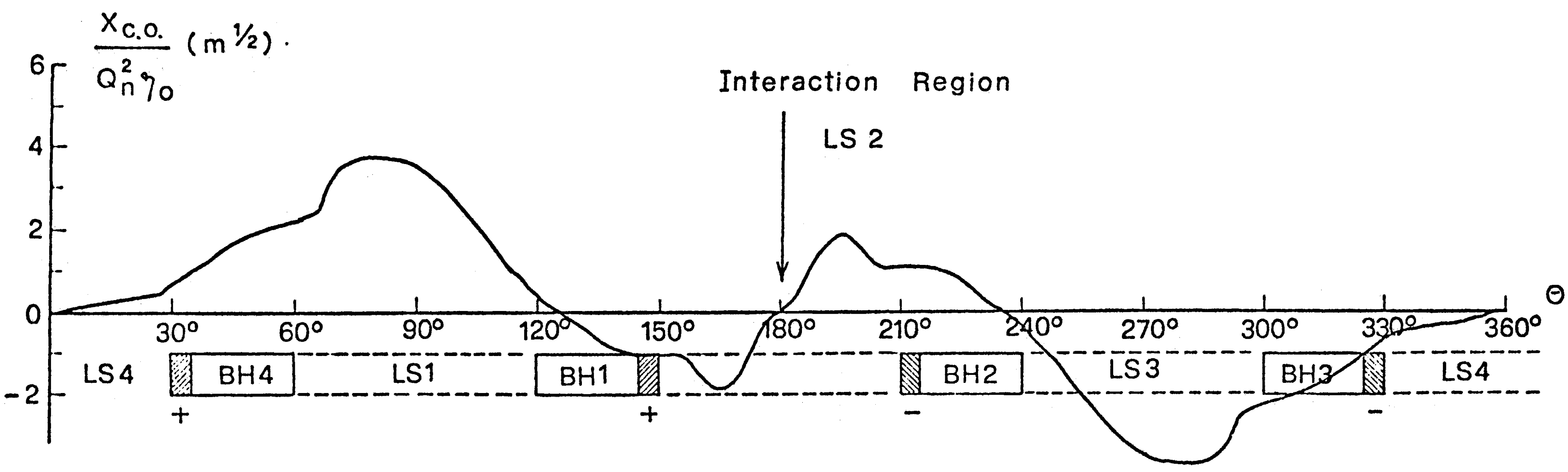

Fig. 5 – Closed orbit pattern

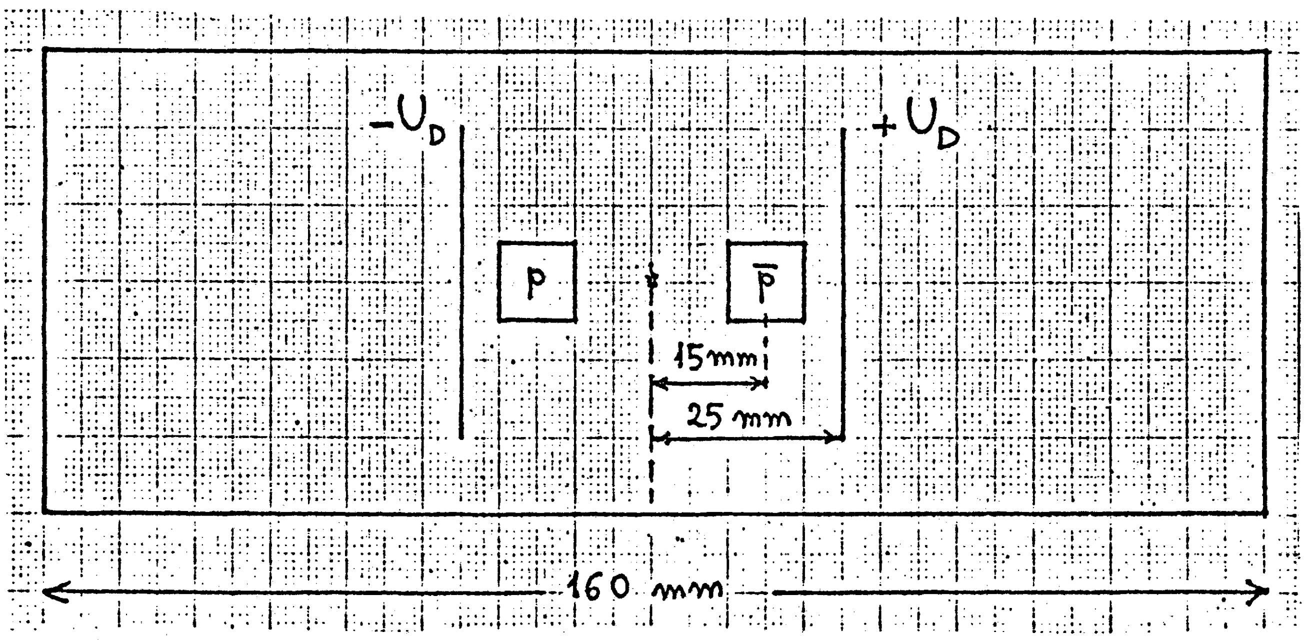

Fig. 6

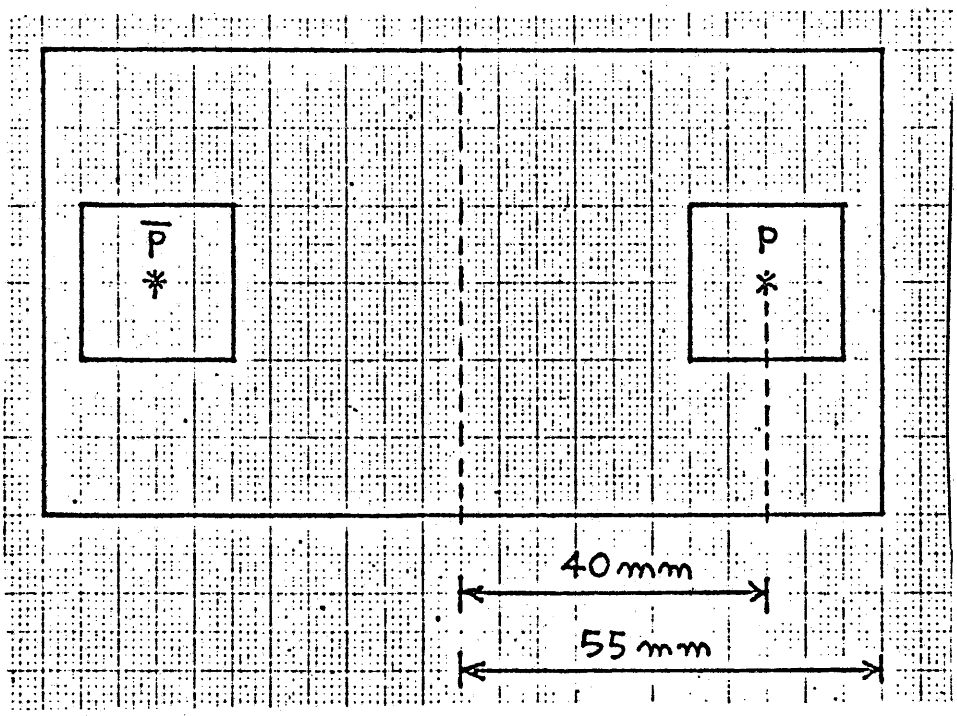

Fig. 7

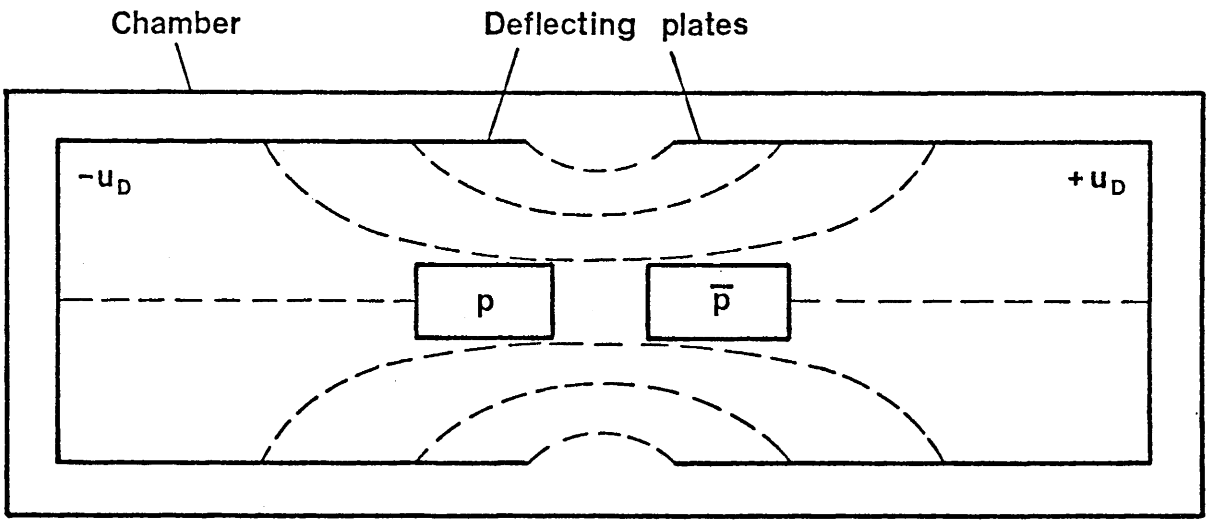

Fig. 8

10.12.81 [signature]